

Quadrupole Relaxation of the ${}^7\text{Li}^+$ Ion in Dilute Aqueous Solution Determined by Experimental and Theoretical Methods

Ralf Baumert*, Ralf Ludwig and Alfons Geiger

Physical Chemistry, University of Dortmund, 44221 Dortmund, Germany (bau@heineken.chemie.uni-dortmund.de)

Received: 15 May 1996 / Accepted: 6 August 1996 / Published: 27 September 1996

Introduction

A combination of molecular dynamics simulations (MD), *ab initio* selfconsistent field (SCF) calculations and nuclear magnetic resonance relaxation time experiments (NMR) is a powerful battery of techniques to investigate the molecular origins of the nuclear quadrupole relaxation mechanism for ${}^7\text{Li}^+$ ions in dilute aqueous solution.

NMR relaxation time experiments for ${}^7\text{Li}^+$ in dilute aqueous solutions can be performed only in the extreme narrowing region. Any quantitative analysis of the measured relaxation rates suffers from the fact that there is no strict separation of the quadrupole coupling constant and the correlation time of the electric field gradient fluctuations at the ${}^7\text{Li}^+$ ion site.

Molecular dynamics simulations allow the calculation of the electric field gradient time correlation function (EFG-TCF). The electric field gradient and the correlation time of the ${}^7\text{Li}^+$ ion can be determined separately and the obtained relaxation rates are compared with experimental data from NMR. The molecular dynamics simulations also provide detailed information about the structure and dynamics of the hydration shell which can not be seen in the experiment. The EFG-TCF is mainly due to the water molecules in the first hydration shell and shows a complex time dependence not describable with a mono-exponential behaviour.

Ab initio self-consistent field (SCF) calculations on molecular clusters from the MD simulation may be a good check for the existence of strong polarizability or many-body effects which are not taken into account in pure electrostatic MD potentials. The MD simulations were used to

generate snapshots of the ${}^7\text{Li}^+$ in aqueous solution (Figure 1) representing the pair correlation function of the whole system. The electric field gradient at the ${}^7\text{Li}^+$ nucleus was then calculated by *ab initio* methods for these configurations and averaged to obtain the quadrupole coupling constant.

NMR relaxation time measurements

The ${}^7\text{Li}^+$ magnetic relaxation time measurements were performed at 360 MHz with the 180 - τ - 90 pulse sequence using a BRUKER AM 360 spectrometer. All measurements were performed on a LiCl solution of the concentration $C^* = 0.555 \text{ m}$ ($\text{m} = \text{aquamolality scale, i.e. moles salt/55.5 moles water}$) which is the same used in the MD studies.

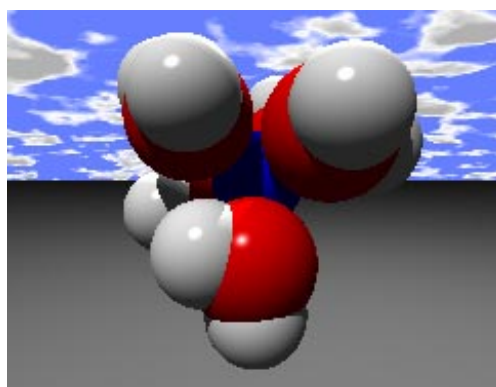


Figure 1. Snapshot from a Molecular Dynamics (MD) Simulation of ${}^7\text{Li}^+$ in water for the first hydration shell.

* To whom correspondence should be addressed

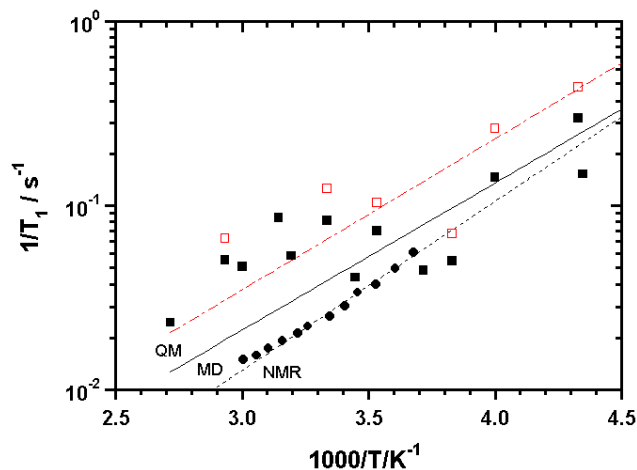


Figure 2. Temperature dependence of lithium relaxation rates from NMR relaxation time experiments (dashed line and filled circles), Molecular Dynamics Simulations (solid line and filled squares) and *ab initio* calculations on MD configurations (dashed-dotted line and open squares).

Beside the desired electric quadrupolar also dipolar interaction contributes to the ${}^7\text{Li}^+$ relaxation rate. A combination of measurements in D_2O and H_2O as well as a correction for the dynamic isotope effect allow the separation of the pure quadrupolar interaction of ${}^7\text{Li}^+$ in water. Our obtained quadrupolar relaxation rates are shown in figure 2. They are comparable with earlier results by Mazitov et. al [1] at a concentration of about 0.2 m. From nmr measurements only, no further conclusion can be drawn. Any quantitative analysis suffers from the fact that there is no strict separation of the quadrupole coupling constant and the correlation time of the electric field gradient fluctuation at the ${}^7\text{Li}^+$ ion site.

$$\text{NMR: } \left(\frac{1}{T_1} \right)_{\text{Li}} = \frac{3}{40} \frac{(2I+3)}{I^2(2I-1)} \left[\frac{eQ}{\hbar} (1 + \gamma_\infty) \right]^2 \bar{V}_{zz}^2 \tau_c$$

Molecular Dynamics simulation

The incontestable advantage of MD compared to experiment and theory is the detailed insight into the system at the molecular level. Therefore quadrupolar relaxation of any free nucleus with spin $I > 1/2$ can be examined by MD, since the strength of the electric field gradient (EFG) is strongly distance dependent and hence only *those* molecules neighbouring the relaxing nucleus have to be taken into account.

Two different mechanisms are discussed as source of the fluctuating field gradient. On the one hand the so called *electronic model* by Deverell [2] supposes that the fluctua-

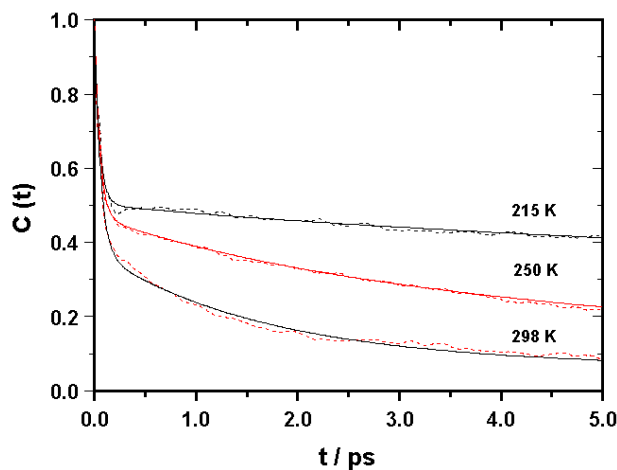


Figure 3. Normalized time correlation functions for the electric field gradient (efg) fluctuations shown for three different temperatures. The solid lines represent the fitted functions for a threefold exponential approach.

tions are due to distortions of the solute electronic cloud by collisions with solvent molecules. On the other hand Hertz [3, 4] and Valiev [5, 6] assume that the *electrostatic* effect of the solvent point dipoles and their thermal motions let arise the fluctuating EFG. Hertz's electrostatic approach has been utilized very successfully to reproduce experimental relaxation rates of different nuclei in a variety of solvents [7]. Consequently this model has already found application in combination with MD-Simulations [8 - 12] because this offers the facility to calculate the mean square amplitude $\langle V_{zz}^2 \rangle$ and the correlation time τ_c separately.

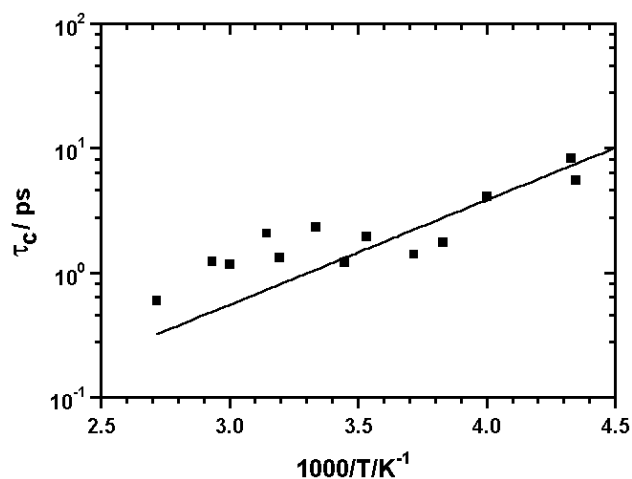


Figure 4. Temperature dependence of the correlation time τ_c of the efg time correlation function (first hydration shell) from MD simulations.

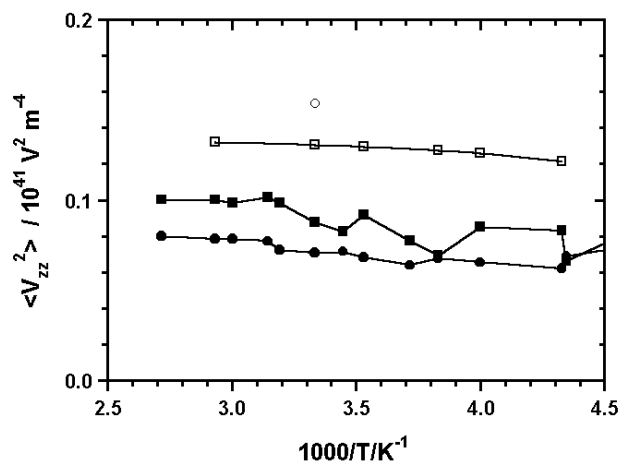


Figure 5. Electric field gradient fluctuations at the ${}^7\text{Li}^+$ position obtained by Molecular Dynamics Simulations (filled symbols) and by *ab initio* calculations on selected clusters from the MD study (open symbols). The squares represent the efg arising from the first hydration shell, the rings show the efg for the full system. For the *ab initio* calculations only the second hydration shell was included. The efg from the MD simulation is already multiplied by the Sternheimer antishielding factor to make the results comparable with the *ab initio* data.

In order to access the NMR-relaxation rates in aqueous solution we performed 15 NVE MD Simulations in the temperature range of $215 \text{ K} \leq T \leq 350 \text{ K}$. With respect to the small system size (100 water molecules + one ion) pbc of a truncated octahedron were applied. To ensure energy conservation Steinhauser-tapering [13] was used with a cut-off radius of 7.868 \AA . Newton's equations of motion were solved by the leap-frog algorithm using a time step of 1 fs . The density has been kept constant at $\rho = 0.997 \text{ g}\cdot\text{cm}^{-3}$. For the water-water interaction the simple point charge (SPC) model was chosen. The water-ion interaction was obtained by applying Lorentz-Berthelot mixing-rules taking the parameter set for ${}^7\text{Li}^+$ of Palinkas et al. [14].

During the initial equilibration run ($\geq 1 \text{ ns}$ for $T \leq 280 \text{ K}$) the temperature was adjusted by the Berendsen-thermostat with a time constant of 0.1 ps . The production runs were performed over 400000 steps (0.4 ns) calculating the EFG-tensor generated by either the whole system or only the first hydration shell at each step. Afterwards $\langle V_{zz}^2 \rangle$ (Figure 5) and the EFG time correlation function (tcf) (Figure 3) up to 20 ps were obtained. The latter show a complex time behaviour that can be described well by a threefold exponential approach. To yield the correlation time τ_c the tcf is integrated up to infinity (Figure 4).

These results - in combination with the Sternheimer factor [15] - reveal access to the relaxation rate.

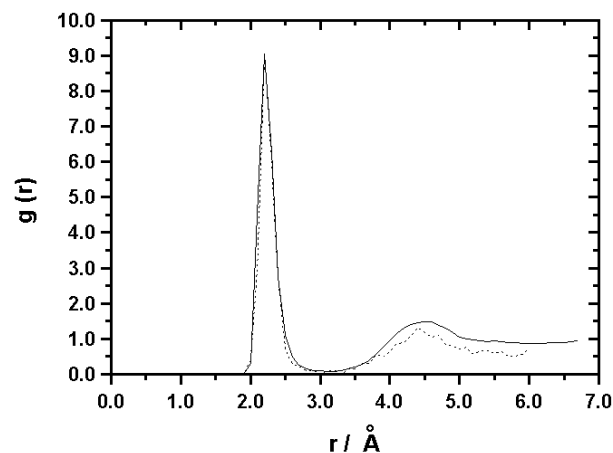


Figure 6. Radial distribution function, $g_{(r)}$, for the oxygen atom relative to lithium (solid line). The dashed line represents the $g_{(r)}$ of one hundred selected MD configurations used for the *ab initio* calculations.

$$\text{MD} : \left(\frac{1}{T_1} \right)_{\text{Li}} = \frac{3}{40} \frac{(2I+3)}{I^2(2I-1)} \left[\frac{eQ}{\hbar} (1 + \gamma_\infty) \right]^2 V_{zz}^2 \tau_c$$

Ab Initio calculations

Equilibrated snapshots of the molecular configurations from MD-simulations were taken at intervals of 4000 steps (4 ps) for six temperatures. In all snapshots a ${}^7\text{Li}^+$ cation is surrounded by a first (4-6 molecules) and a second (30-35 molecules) hydration shell of water molecules. One hundred clusters selected in this way are already able to represent the pair correlation function $g_{\text{Li-O}}$ of the whole system as shown in figure 6. For these clusters *ab initio* cal-

Table 1. Comparison of electric field gradient fluctuations at the ${}^7\text{Li}^+$ position directly obtained from MD simulations and from *ab initio* calculations on MD configurations at 300 K . The efg are listed for MD runs with different system sizes (100, 218 and 400 water molecules). For each simulation the data for the first hydration shell and the total system are shown. In the *ab initio* calculations the efg are calculated including the second hydration shell instead of the full system (results given in $10^{41} \text{ V}^2 \text{ m}^{-4}$).

	100		218		400	
Method	1.HS	2. HS	1.HS	2. HS	1.HS	2. HS
MD	0.0873	0.0705	0.0873	0.0911	0.0858	0.0863
QM	0.1305	0.1535	0.1228	0.1487	0.1101	0.1295

culations were performed on a 6-31+G* basis set [16, 17], Hehre on the Hartree-Fock level of theory to obtain the electric field gradient at the ${}^7\text{Li}^+$ nucleus. In a first set the electric field gradient at ${}^7\text{Li}^+$ caused by the first hydration shell is calculated, in a second set of calculations the influence of the first as well as the second hydration shell is studied. The mean values of the electric field gradient for all chosen clusters are used for comparison with the results obtained directly from Molecular Dynamics Simulations [17, 18] (Figure 5). At 300 K we also investigated whether the efg caused by the first or the first plus the second hydration shell are dependent on the system size in the MD simulations (100, 218 and 400 water molecules). The results obtained by the MD study and the *ab initio* calculations are listed in Table 1.

$$\text{QM: } \left(\frac{1}{T_1} \right)_{\text{Li}} = \frac{3}{40} \frac{(2I+3)}{I^2(2I-1)} \left[\frac{eQ}{\hbar} (1+\gamma_\infty) \right]^2 V_{zz}^2 \tau_c$$

Conclusions

- The pure solvent contribution to the relaxation of lithium in water was studied by NMR relaxation time experiments, Molecular Dynamics Simulations and *ab initio* calculations on MD configurations.

- The electric field gradient correlation functions for all temperatures show a complex time behaviour and can be fitted by a threefold exponential approach.

- The static part \bar{V}_{zz}^2 is a function of the arrangements of the water molecules around lithium. Although the first hydration shell dominates the efg, the influence of outer-sphere waters is significant for all temperatures.

- The differences of the efg's obtained directly from MD simulations and from *ab initio* calculations can be explained by the Sternheimer approximation.

- All electric field gradient fluctuations caused by the first hydration shell as well as the full configuration decrease slightly with decreasing temperature. At lower temperatures the system becomes more structured and the effects of different water molecules will tend to cancel each other.

- In contrast to \bar{V}_{zz}^2 , the correlation time τ_c show great fluctuations with temperature which may require longer simulation runs for better statistics. On the other hand the time correlation functions look reasonable and the simulation runs took already 400 ps.

- In spite of the strong fluctuations with temperature, the activation energies of about 17.6 kJ/mol (MD) and 15.74 kJ/mol (QM) for the lithium relaxation rates are in reasonable agreement with the experimental result of 15.34 kJ/mol. In all cases simple exponential fits for the data were applied although the experimental rates do not strictly follow an Arrhenius-type equation.

References

1. Mazitov, R.; Müller, K.J.; Hertz, H.G. *J. Phys. Chem. NF* **1984**, *140*, 55.
2. Deverell, C. *Mol. Phys.* **1969**, *16*, 491.
3. Hertz, H.G. *Z. Elektrochem.* **1961**, *65*, 20.
4. Hertz, H.G. *Ber. Bunsenges. Phys. Chem.* **1973**, *77*, 531.
5. Valiev, K.A. *Sov. Phys. JETP* **1959**, *37*, 77.
6. Valiev, K.A.; Khabibullin, B.M. *Russ. J. Phys. Chem.* **1961**, *35*, 1118.
7. Weingärtner, H.; Hertz, H.G. *Ber. Bunsenges. Phys. Chem.* **1977**, *81*, 1204.
8. Luhmer, M.; van Belle, D.; Reisse, J.; Odellius, M.; Kowalewski, J.; Laaksonen, A. *J. Chem. Phys.* **1993**, *98*, 2.
9. Schnitker, J.; Geiger, A. *Z. Phys. Chem. NF* **1987**, *155*, 29.
10. Roberts, J.E.; Schnitker, J. *J. Phys. Chem.* **1993**, *97*, 5410.
11. Dejaegere, A.; Luhmer, M.; Stien, M.L.; Reisse, J. *J. Magn. Reson.* **1991**, *91*, 362.
12. Engström, S.; Jönsson, B.; Jönsson, B. *J. Magn. Reson.* **1982**, *50*, 1.
13. Steinhauser, O. *Mol. Phys.* **1982**, *45*, 335.
14. Palinkas, G.; Palinkas, W.O.; Riede, K.; Heinzinger, Z. *Naturforsch.* **1977**, *32a*, 1137.
15. Sternheimer, R.M. *Phys. Rev.* **1966**, *146*, 140.
16. Gaussian 92, Revision A, M. J. Frisch, G. W. Trucks, M. Head-Gordon, P.M.W. Gill, M. W. Wong, J.B. Foresman, B. G. Johnson, H. B. Schlegel, M.A. Robb, E.S. Replogle, R. Gomperts, J.L. Andres, K. Raghavachari, J.S. Binkley, C. Gonzalez, R.L. Martin, D.J. Fox, D.J. Defrees, J. Baker, J.J.P. Steward, and J. A. Pople, Gaussian, Inc., Pittsburgh, PA, 1992.
17. Eggenberger, R.; Gerber, S.; Huber, H.; Searles, D. and Welker, M. *J. Chem. Phys.* **1992**, *97*, 5898.
18. Eggenberger, R.; Gerber, S.; Huber, H.; Searles, D. and Welker, M. *Mol. Phys.* **1993**, *80*, 1177.